

# Uniaxial pressure effects on the unusual antiferromagnetic transition in the Kondo semiconductor $\text{CeOs}_2\text{Al}_{10}$

Kyosuke Hayashi<sup>1</sup>, Kazunori Umeo<sup>1,2,\*</sup>, Yoshihiro Yamada<sup>1</sup>, Jo Kawabata<sup>1</sup>, Yuji Muro<sup>4</sup>, and Toshiro Takabatake<sup>1,3</sup>

<sup>1</sup> Graduate School of Advanced Sciences of Matter, Hiroshima University, Higashi-Hiroshima, Hiroshima 739-8530, Japan

<sup>2</sup> Cryogenics and Instrumental Analysis Division, N-BARD, Hiroshima University, Higashi-Hiroshima, Hiroshima 739-8526, Japan

<sup>3</sup> Institute for Advanced Materials Research, Hiroshima University, Higashi-Hiroshima, Hiroshima 739-8530, Japan

<sup>4</sup> Department of Intelligent Systems Design Engineering, Faculty of Engineering, Toyama Prefectural University, Imizu, Toyama 939-0398, Japan

E-mail: kumeo@sci.hiroshima-u.ac.jp

**Abstract.** We have studied the relation between the unusual antiferromagnetic (AFM) ordering and anisotropic  $c$ - $f$  hybridization in  $\text{CeOs}_2\text{Al}_{10}$  by measuring the magnetic susceptibility  $\chi$  under uniaxial pressures  $P$  up to 0.45 GPa. For  $P \parallel B \parallel a$  and  $P \parallel B \parallel c$ , the AFM ordering temperature  $T_N = 28.5$  K hardly changes with increasing  $P$ , while the value of  $\chi$  decreases and the maximal temperature  $T_\chi^{\text{max}}$  of  $\chi(T)$  shifts to higher temperatures. These findings suggest that the intensity of  $c$ - $f$  hybridization is enhanced along the pressurized  $a$  and  $c$  axes. On the other hand, for  $P \parallel b$ ,  $T_N$  increases up to 30 K at 0.15 GPa, while the value of  $\chi$  remains unchanged. This observation for  $P \parallel b$  suggests that the net intensity of  $c$ - $f$  hybridization decreases, while the  $c$ - $f$  hybridization along the  $b$ -axis hardly changes. We discuss these results in terms of the atomic displacements of Os, Al(3) and Al(4) under uniaxial pressures.

## 1. Introduction

Cerium based intermetallic compounds display rich physical properties, such as, heavy-fermion state, unusual magnetically ordered state, and semiconducting state, which arise from the hybridization between the conduction electrons and localized  $4f$  electrons, namely,  $c$ - $f$  hybridization. Among these compounds,  $\text{CeNiSn}$  and  $\text{CeRhSb}$ , so called Kondo semiconductors, possess an anisotropic (pseudo) gap in the density of states at the Fermi level due to the anisotropic  $c$ - $f$  hybridization [1]. In fact, applying uniaxial pressure on  $\text{CeNiSn}$  along the orthorhombic  $a$ -axis enhances the  $c$ - $f$  hybridization, increasing the gap magnitude [2].

The conventional Kondo semiconductors did not exhibit magnetic ordering because of the strong  $c$ - $f$  hybridization. However, it has been established that  $\text{CeT}_2\text{Al}_{10}$  ( $T = \text{Ru, Os}$ ) exhibit both Kondo semiconducting behavior and antiferromagnetic (AFM) orders at  $T_N = 27.3$  and  $28.5$  K, respectively [3–8]. Both compounds crystallize in the orthorhombic  $\text{YbFe}_2\text{Al}_{10}$ -type structure, in which Ce and T atoms form a zigzag chain along the  $c$ -axis as shown in Fig. 1. The easy magnetization axis is the  $a$ -axis in the paramagnetic state, while the AFM ordered moment  $\mu_{\text{AFM}}$  is oriented parallel to the  $c$ -axis. Although the



magnitudes of  $\mu_{\text{AFM}}$  of  $0.3\sim 0.4\mu_{\text{B}}/\text{Ce}$  in  $\text{CeT}_2\text{Al}_{10}$  are smaller than  $7\mu_{\text{B}}/\text{Gd}$  for  $\text{GdT}_2\text{Al}_{10}$ ,  $T_{\text{N}}$ 's in the Ce compounds are higher than those in the Gd counterparts, respectively [9,10]. An optical conductivity study has suggested that the unusual AFM order is induced by the formation of charge density wave occurring along the  $b$ -axis [11]. In spite of intensive works, the origin of the AFM order remains unsolved yet.

The analyses of the magnetic susceptibility by crystal field model and of polarization-dependent soft x-ray absorption spectra of  $\text{CeT}_2\text{Al}_{10}$  have revealed that the Ce  $4f$  wave function lies in the  $b$ - $c$  plane [12,13]. It suggested that the hybridization between the Ce  $4f$  electrons and Al  $3p$  electrons is important for the unusual AFM. Furthermore, for  $\text{CeRu}_2\text{Al}_{10-y}\text{Si}_y$ , the  $T_{\text{N}}$  and the absolute value of paramagnetic Curie temperature  $|\theta_{\text{p}}|$  decrease with increasing  $y$ . The decreases in  $T_{\text{N}}$  and  $|\theta_{\text{p}}|$  with  $y$  coincide with those reported in the  $4d$  electron doped system  $\text{Ce}(\text{Ru}_{1-x}\text{Rh}_x)_2\text{Al}_{10}$  with respect to the number of doped electrons per formula unit. This coincidence indicates that the Ru  $4d$ - and Al  $3p$ - electrons in  $\text{CeRu}_2\text{Al}_{10}$  play the equivalent role in the unusual AFM order [14,15]. Namely, the hybridization of the Ce  $4f$  electrons with the  $4d$ - $3p$  hybridized conduction band is essential in AFM order in  $\text{CeRu}_2\text{Al}_{10}$  [16]. On the other hand, the variations of lattice parameters in the series of  $\text{LnT}_2\text{Al}_{10}$  (Ln = lanthanides, T = Fe, Ru, Os) suggested that the intensity of the  $c$ - $f$  hybridization is stronger in the  $a$ - $c$  plane than that along the  $b$ -axis [10,17].

In order to examine the relation between the unusual AFM order and  $c$ - $f$  hybridization, the pressure effects on the resistivity and magnetic susceptibility  $\chi$  of  $\text{CeOs}_2\text{Al}_{10}$  have been investigated previously [18]. The  $T_{\text{N}}$  of  $\text{CeOs}_2\text{Al}_{10}$  reached a maximum of 29 K at 0.7 GPa, and suddenly disappeared at  $P_{\text{c}} = 2.5$  GPa. On the other hand, the maximal temperature in  $\chi(T)$ , which is proportional to the Kondo temperature, increased linearly with pressure. However, hydrostatic pressure studies provided little information of the role of the anisotropic  $c$ - $f$  hybridization in the unusual AFM order, because the contraction under hydrostatic pressures is almost isotropic for  $P < P_{\text{c}}$  [19]. In order to obtain clearer information, we have measured the magnetization under the uniaxial pressures along the principal axes.

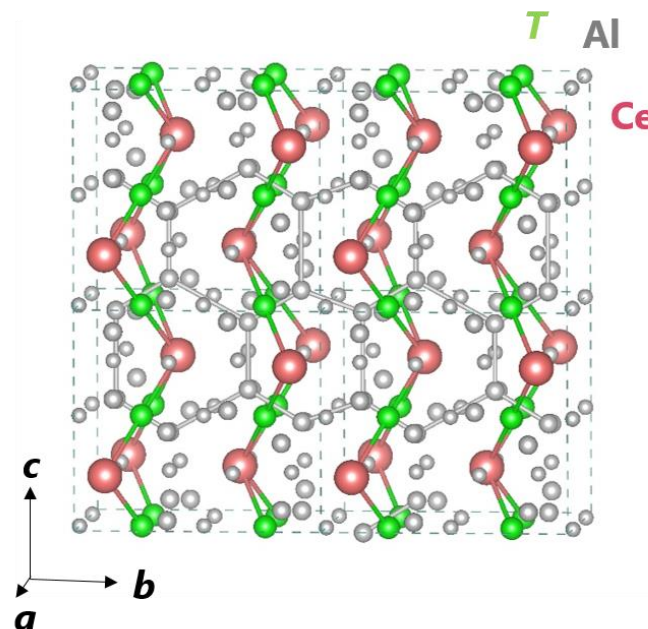


**Figure 1.** Crystal structure of  $\text{CeT}_2\text{Al}_{10}$  [11].

## 2. Experiment

Single-crystalline samples of  $\text{CeOs}_2\text{Al}_{10}$  were grown using an Al self-flux method as described previously [6]. Powder x-ray diffraction patterns of the samples confirmed the  $\text{YbFe}_2\text{Al}_{10}$ -type structure. The samples were cut into plates of the width of 0.5 ~ 0.8 mm with the masses of 8 ~ 15 mg for  $P \parallel a$  and  $P \parallel c$  and 25 mg for  $P \parallel b$ , respectively. The sample plate was sandwiched between  $\text{ZrO}_2$  pistons in the homemade pressure cell. The magnetization was measured by using a commercial superconducting quantum interference device magnetometer (Quantum Design MPMS) at a magnetic field  $B = 4$  T in the temperature range from 2 to 300 K. The direction of the uniaxial pressure  $P$  is always parallel to  $B$ . The pressure was determined by the known pressure dependence of the superconducting transition temperature of tin.

## 3. Results and Discussion

Figure 2 shows the temperature dependence of the magnetic susceptibility  $\chi$  of  $\text{CeOs}_2\text{Al}_{10}$ . The values of  $\chi$  for  $P \parallel a$  and  $P \parallel c$  decrease with pressure. On the other hand, the value of  $\chi$  for  $P \parallel b$  hardly changes for  $P \leq 0.15$  GPa, while it slightly decreases for  $P \geq 0.2$  GPa as shown in the inset of Fig. 2 (b). Furthermore, maximal temperatures  $T_\chi^{\text{max}}$  of  $\chi(T)$  increase from 43 K at 0 GPa up to 48 K at  $P \parallel a = 0.45$  GPa and to 50 K at  $P \parallel c = 0.31$  GPa.

In order to examine the pressure dependence of  $T_N$  for  $P \parallel a$ , we plot the  $d(\chi T)/dT$  vs  $T$  in Figure 3 (a). The peak temperatures of  $d(\chi T)/dT$  do not change up to 0.45 GPa. Moreover, for  $P \parallel c$ , the anomaly in  $\chi(T)$  due to the AFM order also hardly changes as shown in Fig. 3 (b). However, as shown in Fig. 4, for  $P \parallel b$ , the  $T_N$  increases up to 0.15 GPa and decreases for  $P > 0.15$  GPa.

Figure 5 shows the dependences of  $T_N$  of  $\text{CeOs}_2\text{Al}_{10}$  on uniaxial pressures and hydrostatic pressure. The inset displays the pressure dependence of  $T_\chi^{\text{max}}$ . For  $P \parallel b$ ,  $T_N$  increases up to 30 K at 0.15 GPa,

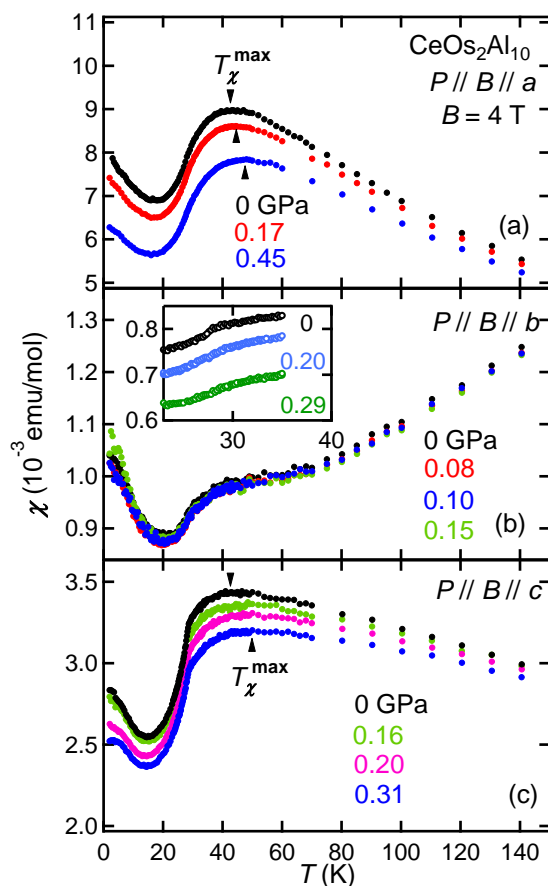


Figure 2. Temperature dependence of the magnetic susceptibility  $\chi$  of  $\text{CeOs}_2\text{Al}_{10}$  under uniaxial pressures. The inset in Fig. 2 (b) shows the shifted data at around  $T_N$  for  $P \parallel b > 0.2$  GPa.

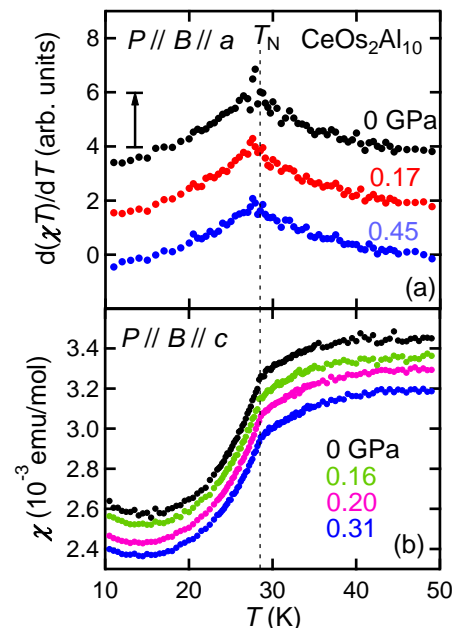


Figure 3. Temperature dependence of the  $d(\chi T)/dT$  for  $P \parallel B \parallel a$  (a) and  $\chi(T)$  for  $P \parallel B \parallel c$  (b) of  $\text{CeOs}_2\text{Al}_{10}$ .

while  $T_N$  does not change for  $P \parallel a$  and  $P \parallel c$ . This maximum of  $T_N = 30$  K is higher than  $T_N = 29$  K under the hydrostatic pressure of 0.7 GPa. Furthermore, the values of  $dT_N^{\max}/dP$  for  $P \parallel a$  and  $P \parallel c$  are 11 K/GPa and 23 K/GPa, respectively, which are larger than those of 7 K/GPa and 11 K/GPa for  $\chi_a$  and  $\chi_c$  under the hydrostatic pressure [18].

We obtained two important results: (i) for  $P \parallel a$  and  $P \parallel c$ ,  $T_N$  does not change, although the  $c$ - $f$  hybridizations along the pressurized direction become stronger. (ii) for  $P \parallel b$ ,  $T_N$  rises, whereas the  $c$ - $f$  hybridizations along  $b$ -axis hardly changes. We discuss these results by considering the atomic displacement under uniaxial pressures as shown in Fig. 6. Here, we consider the hybridization among the Os 5d, Al(3), Al(4) 3p and Ce 4f charge cloud, because the 4f charge is distributed mainly in the  $b$ - $c$  plane [12,13]. For simplicity, the Al(3) is not drawn in Fig. 6 (b – d), because Al(3) seems to move to the same direction of Al(4). First, we discuss (i). Applying pressure along the  $a$ -axis causes the extension of the lattice along the  $b$ -axis and  $c$ -axis. Here, we will consider the atomic displacement in the  $a$ - $c$  plane, because the intensity of  $c$ - $f$  hybridization along the  $b$ -axis is insensitive to the change in the  $b$ -axial length. One expects that each atom move along the arrows as shown in Fig. 6 (b). In this situation, the Os atoms approach to the 4f charge cloud and the Al atoms move away from the Ce atom to the directions of arrows. The, the  $c$ - $f$  hybridization in the  $a$ - $c$  plane may hardly change, because the change of distance between the Os 5d - Al 3p hybridized charge cloud and the Ce 4f charge cloud is small. For  $P \parallel c$ , as shown in Fig. 6 (c), Os and Al move to opposite directions to that for  $P \parallel a$ . Thus, the  $c$ - $f$  hybridization in the  $a$ - $c$  plane also may be constant. Therefore,  $T_N$  hardly changes for  $P \parallel a$  and  $P \parallel c$ . On the other hand, for  $P \parallel b$ , both Os and Al would move away from the 4f charge cloud as shown in Fig. 6 (d). Thus, the hybridization between the Os 5d - Al 3p hybridized charge cloud and Ce 4f charge cloud is weakened, which results in the rise in  $T_N$ .

As we noted above, the hybridization between the Os 5d - Al(3), Al(4) 3p electrons and Ce 4f electron should play an important role in the unusual AFM order in  $\text{CeOs}_2\text{Al}_{10}$ . To confirm this scenario, we plan to measure the magnetization in the configuration  $P \perp B$ .

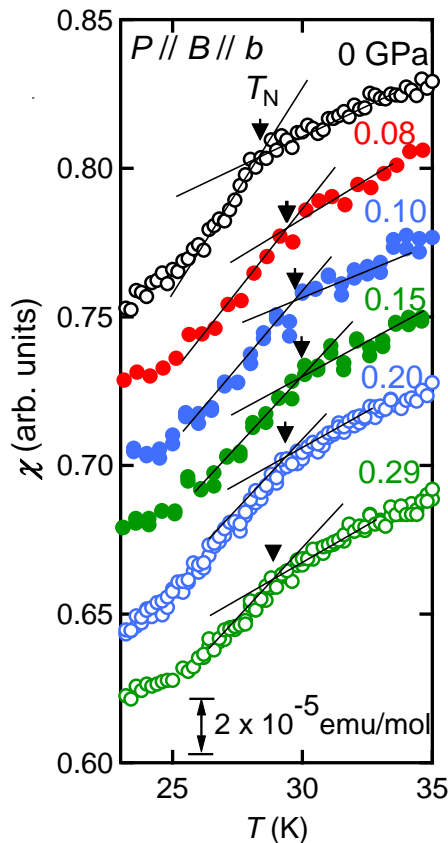


Figure 4.  $\chi(T)$  for  $P \parallel B \parallel b$ .  $T_N$  was defined as the cross-point of the two lines as depicted in the figure.

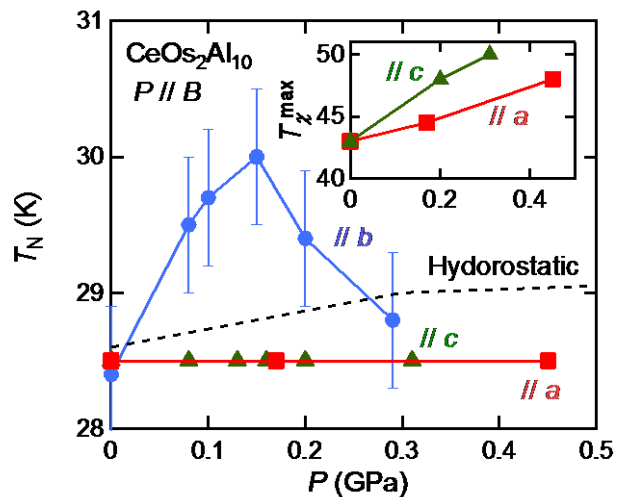


Figure 5. Pressure dependence of  $T_N$  of  $\text{CeOs}_2\text{Al}_{10}$  for uniaxial and hydrostatic pressures [18]. The inset shows the pressure dependence of the maximal temperature of  $\chi(T)$ .

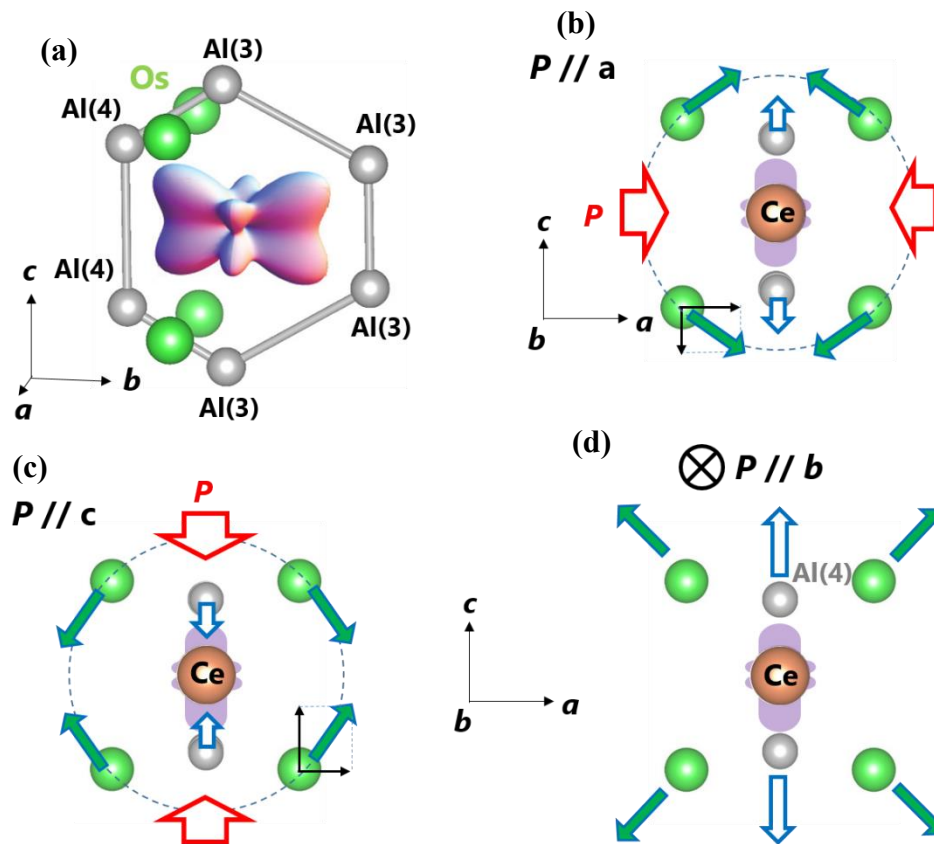


Figure 6. (a) Charge distribution of Ce 4f electrons in CeOs<sub>2</sub>Al<sub>10</sub> [12,13]. (b – d) Displacements of Os and Al (4) under uniaxial pressures  $P // a$  (b),  $P // c$  (c) and  $P // b$  (d), respectively, viewed from the  $b$ -direction.

### Acknowledgements

The magnetization measurements under uniaxial pressures were performed at N-BARD, Hiroshima University. This work was partly supported by KAKENHI Grant Numbers Nos. 25400375, 26400363 and 16H01076.

### References

- [1] Takabatake T, Teshima F, Fujii H, Nishigori S, Suzuki T, Fujita T, Yamaguchi Y, Sakurai J and Jaccard D 1990 *Phys. Rev. B* **41** 9607
- [2] Umeo K, Igaue T, Chyono H, Echizen Y, Takabatake T, Kosaka M and Uwatoko Y 1999 *Phys. Rev. B* **60** R6957
- [3] Thiede V M T, Edel T and Jeitschko W 1998 *J. Mater. Chem.* **8** 125
- [4] Muro Y, Motoya K, Saiga Y and Takabatake T 2010 *J. Phys. Conf. Ser.* **200** 012136
- [5] Nishioka T, Kawamura Y, Takesawa T, Kobayashi R, Kato H, Matsumura M, Kodama K, Matsubayashi K and Uwatoko Y 2009 *J. Phys. Soc. Jpn.* **78** 123705
- [6] Muro Y, Umeo K, Nishimoto K, Tamura R and Takabatake T 2010 *Phys. Rev. B* **81** 214401
- [7] Khalyavin D D, Hillier A D, Adroja D T, Strydom A M, Manuel P, Chapon L C, Peratheepan P, Knight K, Deen P, Ritter C, Muro Y and Takabatake T 2010 *Phys. Rev. B* **82** 100405 (R)
- [8] Kato H, Kobayashi R, Takesaka T, Nishioka T, Matsumura M, Kaneko K and Metoki N 2011

*J. Phys. Soc. Jpn.* **80** 073701

- [9] Morrison G, Haldolaarachchige N, P Young D and Chan J Y 2012 *Condens. Matter* 356002
- [10] Muro Y, Kajino J, Onimaru T and Takabatake T 2011 *J. Phys. Soc. Jpn.* **80** SA021
- [11] Kimura S, Iizuka T, Miyazaki H, Hajiri T, Matsunami M, Mori T, Irizawa A, Muro Y, Kajino J and Takabatake T 2011 *Phys. Rev. B* **84** 165125
- [12] Yutani K, Muro Y, Kajino J, Sato T J and Takabatake T 2012 *J. Phys. Conf. Ser.* **391** 012070
- [13] Strigari F, Willers T, Muro Y, Yutani K, Takabatake T, Hu Z, Agrestini S, Kuo C Y, Chin Y Y, Lin H J, Pi T W, Chen C T, Weschke E, Schierle E, Tanaka A, Haverkort M W, Tjeng L H and Severing A 2013 *Phys. Rev. B* **87** 125119
- [14] Kobayashi R, Ogane Y, Hirai D, Nishioka T, Matsumura M, Kawamura Y, Matsubayashi K, Uwatoko Y, Tanida H and Sera M 2013 *J. Phys. Soc. Jpn.* **82** 093702
- [15] Muro Y, Hida K, Fukuhara T, Kawabata J, Yutani K and Takabatake T 2014 *JPS Conf. Proc.* **3** 012017
- [16] Hayashi K, Muro Y, Fukuhara T, Kawabata J, Kuwai T and Takabatake T 2016 *J. Phys. Soc. Jpn.* **85** 034714
- [17] Sera M, Tanaka D, Tanida H, Moriyoshi C, Ogawa M, Kuroiwa Y, Nishioka T, Matsumura M, Kim J, Tsuji N and Tanaka M 2013 *J. Phys. Soc. Jpn.* **82** 024603
- [18] Umeo K, Ohsuka T, Muro Y, Kajino J and Takabatake T 2011 *J. Phys. Soc. Jpn.* **80** 064709
- [19] Kawamura Y, Hayashi J, Takeda K, Sekine C, Tanida H, Sera M and Nishioka T 2016 *J. Phys. Soc. Jpn.* **85** 044601